Article

Cell Reports

Hepatic mTORC1 Opposes Impaired Insulin Action to Control Mitochondrial Metabolism in Obesity

Graphical Abstract

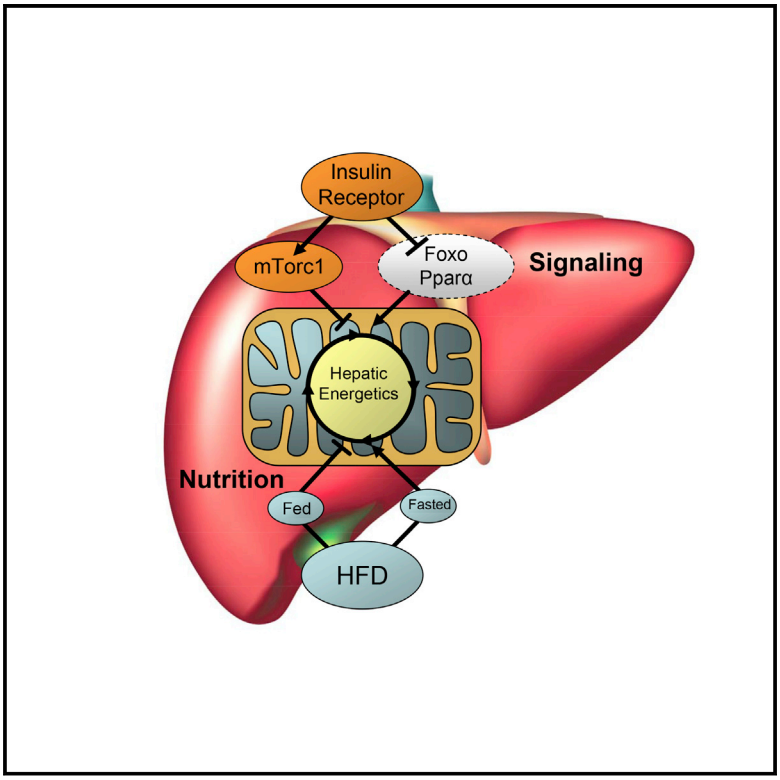

Authors

Blanka Kucejova, Joao Duarte, Santhosh Satapati, ..., Christopher B. Newgard, James Brugarolas, Shawn C. Burgess

Correspondence

shawn.burgess@utsouthwestern.edu

In Brief

Using in vivo stable isotope tracers, Kucejova et al. find that loss of hepatic insulin action stimulates mitochondrial metabolism and that activation of mTORC1 suppresses mitochondrial metabolism and decreases nutritional flexibility. Together, loss of insulin action and activation of mTORC1 recapitulate certain effects of diet-induced insulin resistance on mitochondrial metabolism.

Highlights

- Loss of the hepatic insulin receptor (IR) stimulates oxidative metabolism in liver
- Activation of mTORC1 suppresses oxidative metabolism in liver
- Simultaneous IR loss and mTORC1 activation cause hyperglycemia and impaired ketosis

Kucejova et al., 2016, Cell Reports *16*, 508–519
July 12, 2016
http://dx.doi.org/10.1016/j.celrep.2016.06.006

OPEN ACCESS
CellPress

Cell Reports
Article

Hepatic mTORC1 Opposes Impaired Insulin Action to Control Mitochondrial Metabolism in Obesity

Blanka Kucejova,[1] Joao Duarte,[1] Santhosh Satapati,[1] Xiaorong Fu,[1] Olga Ilkayeva,[5] Christopher B. Newgard,[5] James Brugarolas,[3,4] and Shawn C. Burgess[1,2,*]
[1]AIRC Division of Metabolic Mechanisms of Disease
[2]Department of Pharmacology
[3]Kidney Cancer Program, Simmons Comprehensive Cancer Center
[4]Department of Internal Medicine
The University of Texas Southwestern Medical Center, Dallas, TX 75390, USA
[5]Sarah W. Stedman Nutrition and Metabolism Center and Duke Molecular Physiology Institute, Department of Pharmacology and Cancer Biology and Department of Medicine, Duke University Medical Center, Durham, NC 27710, USA
*Correspondence: shawn.burgess@utsouthwestern.edu
http://dx.doi.org/10.1016/j.celrep.2016.06.006

SUMMARY

Dysregulated mitochondrial metabolism during hepatic insulin resistance may contribute to pathophysiologies ranging from elevated glucose production to hepatocellular oxidative stress and inflammation. Given that obesity impairs insulin action but paradoxically activates mTORC1, we tested whether insulin action and mammalian target of rapamycin complex 1 (mTORC1) contribute to altered in vivo hepatic mitochondrial metabolism. Loss of hepatic insulin action for 2 weeks caused increased gluconeogenesis, mitochondrial anaplerosis, tricarboxylic acid (TCA) cycle oxidation, and ketogenesis. However, activation of mTORC1, induced by the loss of hepatic *Tsc1*, suppressed these fluxes. Only glycogen synthesis was impaired by both loss of insulin receptor and mTORC1 activation. Mice with a double knockout of the insulin receptor and *Tsc1* had larger livers, hyperglycemia, severely impaired glycogen storage, and suppressed ketogenesis, as compared to those with loss of the liver insulin receptor alone. Thus, activation of hepatic mTORC1 opposes the catabolic effects of impaired insulin action under some nutritional states.

INTRODUCTION

Hepatic insulin resistance is a key factor in many pathophysiologies of obesity, including diabetes and nonalcoholic fatty liver disease (NAFLD). Defects in hepatic insulin signaling contribute to poor glycemia by causing inadequate phosphorylation of Foxo transcription factors that regulate gluconeogenesis and by ineffectively modulating the phosphorylation of glycogen synthase and glycogen phosphorylase (Lin and Accili, 2011). Metabolic pathways that promote liver damage are also initiated by loss of the insulin signaling, perhaps through effects on oxidative metabolism (Haas et al., 2012) and oxidative damage (Michael et al., 2000). Activation of oxidative metabolism in the liver of obese humans (Iozzo et al., 2010; Sunny et al., 2011) suggests a similar mechanism in NAFLD subjects. Inasmuch as inhibiting pathways associated with the tricarboxylic acid (TCA) cycle protects against hepatic oxidative stress and inflammation in mice (Satapati et al., 2015), oxidative metabolism appears to play a critical role in the progression of NAFLD.

Chronic exposure to obesity eventually causes defects in hepatic mitochondrial function (Mantena et al., 2009; Rector et al., 2010; Thyfault et al., 2009), but some aspects of mitochondrial metabolism may be altered prior to damage in response to disruptions in insulin signaling. For example, despite insulin resistance, insulin signaling over-activates hepatic lipogenesis (Shimomura et al., 2000), a pathway normally antithetic to fat oxidation. This "selective insulin resistance" occurs with the paradoxical activation of signaling proteins downstream of the insulin receptor. Specifically, mammalian target of rapamycin complex 1 (mTORC1), a serine-threonine protein kinase with broad roles in cell growth, replication, survival, aging, and metabolism (Howell et al., 2013; Zoncu et al., 2011), lies downstream of the insulin receptor and is required for elevated lipogenesis during insulin resistance (Li et al., 2010). Importantly, mTORC1 target proteins may also act to suppress the expression of gluconeogenic (Lustig et al., 2011) and ketogenic genes in liver (Sengupta et al., 2010). A key challenge for understanding the molecular metabolism of insulin resistance is to determine how downstream signaling nodes, like mTORC1, function to regulate metabolic flux, particularly in mitochondria.

To test the hypothesis that hepatic mitochondrial metabolism is altered by signaling components of insulin resistance, we studied loss of insulin action and activation of mTORC1. Stable isotope tracers were used to evaluate in vivo metabolic flux in mice that were either fed chow or an 8-week high-fat diet (HFD) after an acute (2-week) loss of the insulin receptor and/or constitutive activation of mTORC1 by loss of *Tsc1* (Kwiatkowski et al., 2002). We report that loss of insulin action stimulated hepatic TCA cycle metabolism and fat oxidation, similar to our

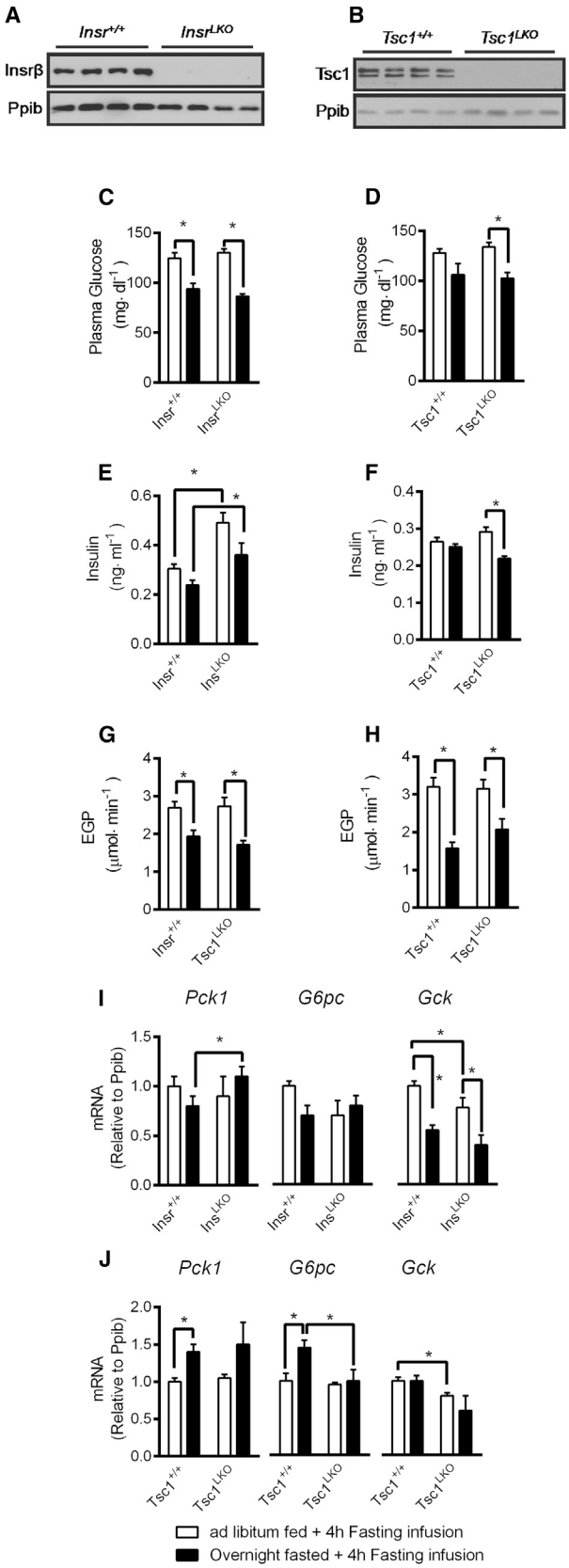

Figure 1. Characteristics of Mice Fed a Chow Diet with Short-Term Hepatic *Tsc1* or *Insrβ* Removal

Mice on a chow diet (n = 4–7) were fed ad libitum or overnight (17 hr) fasted prior to tracer infusions.

(A and B) Western blot analyses for Insrβ (A) and Tsc1 (B) proteins in liver lysates from animals sacrificed 14 days after Ad-Cre injection.

(C and D) Blood glucose concentration in $Insr^{LKO}$ (C) and $Tsc1^{LKO}$ (D) mice.

(E and F) Plasma insulin concentration in $Insr^{LKO}$ (E) and $Tsc1^{LKO}$ (F) mice.

(G and H) Endogenous glucose production measured by [3,4-^{13}C]glucose turnover in $Insr^{LKO}$ (G) and $Tsc1^{LKO}$ (H) mice.

(I and J) qRT-PCR analysis of genes related to glucose metabolism in $Insr^{LKO}$ (I) and $Tsc1^{LKO}$ (J) liver.

All parameters except blood glucose were analyzed after the end of infusion, which required an additional ~4-hr fast. Data are expressed as the mean and SE, with significant differences determined by unpaired two-tailed Student's t test assuming equal variances and identified as *$p < 0.05$.

previous findings in fasted mice after 16 weeks of an HFD (Satapati et al., 2012). In contrast, a shorter (8-week) HFD suppressed TCA cycle metabolism in fed mice, resulting in a blunted fed-to-fasted increment in the flux. This effect was recapitulated by mTORC1 activation. Glycogen metabolism was impaired by both the loss of insulin receptor and activation of mTORC1. Activation of mTORC1 in insulin receptor knockout (KO) liver further provoked hyperglycemia, worsened glycogen storage, and suppressed fasting ketosis. Hence, loss of insulin action excited mitochondrial metabolism, but mTORC1 activation suppressed mitochondrial metabolism, and, together, they caused hyperglycemia with impaired hepatic fat oxidation, a combination observed in severe diabetic models.

RESULTS

Short-Term Liver-Specific *Tsc1* and *Insrβ* Deletion Have Opposite Effects on Hepatic Gluconeogenesis in Mice

To study the heterogeneous metabolic effects of loss of insulin action and constitutive mTORC1 activation, we examined mice with conditional loss of hepatic *Insrβ* or *Tsc1* for glucose homeostasis (Figure 1). Liver-specific removal was mediated by Ad-Cre (adenovirus coding for Cre recombinase) recombination of floxed alleles in adult $Tsc1^{F/F}$ (Tsc^{LKO}) and $Insr\beta^{F/F}$ ($Insr^{LKO}$) mice 2 weeks prior to experiments to minimize adaptive effects due to long-term hepatic inactivation of *Tsc1* (Kwiatkowski et al., 2002) or *Insrβ* (Michael et al., 2000). Ad-Cre treatment led to ~90% *Tsc1* and *Insrβ* knockdown (Figures 1A and 1B). To account for the effect of Cre recombinase expression and adenovirus infection, all control mice were injected with Ad-Cre.

The metabolic effects of *Insrβ* loss or mTORC1 gain of function were first examined in mice fed a chow diet after an ~4-hr (fed/postabsorptive) or 24-hr (fasted) fast. Both genotypes had normal plasma glucose concentrations in the fed and fasted states (Figures 1C and D). However, insulin concentration was significantly increased in the $Insr^{LKO}$ mice (Figure 1E) but not the Tsc^{LKO} mice (Figure 1F). To clarify whether 2 weeks of inactivation of the insulin receptor or activation of mTORC1 is sufficient to alter glucose homeostasis, we performed tracer studies of endogenous glucose production (EGP). Glucose production was significantly reduced in fasted mice compared to fed mice, but neither loss of hepatic insulin receptor (Figure 1G) nor activation of mTORC1 (Figure 1H) altered EGP. Despite

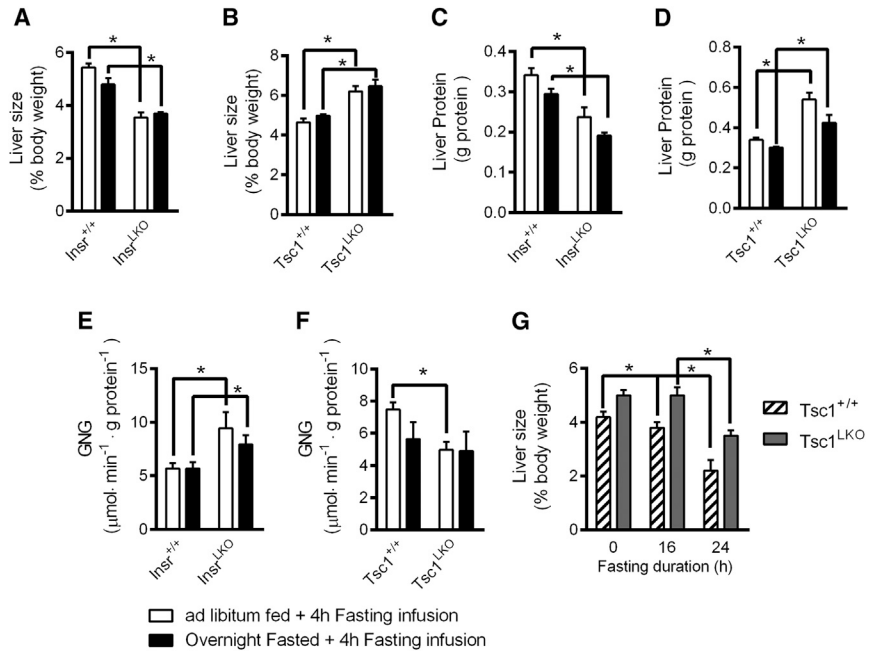

Figure 2. Hepatocellular Gluconeogenesis Is Induced by Loss of Insulin Action and Suppressed by mTORC1 Activation

Mice on a chow diet (n = 4–7) were fed ad libitum or overnight (17 hr) fasted.

(A and B) Liver:body weight in $Insr^{LKO}$ (A) and $Tsc1^{LKO}$ (B) mice.

(C and D) Total liver protein content in $Insr^{LKO}$ (C) and $Tsc1^{LKO}$ (D) mice.

(E–G) Since liver size was dramatically altered by loss of *Insr* and *Tsc1*, gluconeogenic (GNG) flux in $Insr^{LKO}$ (E) and $Tsc1^{LKO}$ (F) mice was measured by ^{2}H incorporation into plasma glucose H2 and H5, and expressed in μmol · min^{-1} · g liver $protein^{-1}$. (G) Liver:body weight during a 24-hr fast in $Tsc1^{LKO}$ mice.

All parameters were analyzed after the end of the infusion, which required an additional ~4-hr fast. Data are expressed as the mean and SE, with significant differences determined by unpaired two-tailed Student's t test assuming equal variances and identified as *$p < 0.05$.

normal rates of glucose production, liver mRNA levels of several enzymes of glucose metabolism were altered. *Pck1* expression (cytosolic phosphoenolpyruvate carboxykinase) was increased, and *Gck* (glucokinase) was decreased in the liver of $Insr^{LKO}$ mice (Figure 1I). These genes were expressed at relatively normal or reduced expression in $Tsc1^{LKO}$ mice on a chow diet (Figure 1J) or an HFD.

Since the insulin signaling pathway partially mediates growth, we examined whether liver size was altered in $Insr^{LKO}$ or $Tsc1^{LKO}$ mice (Figure 2). The liver:body ratio was decreased by 35% after the loss of insulin receptor (Figure 2A) but increased by 35% after mTORC1 activation (Figure 2B). The change in liver mass (Tables S1 and S2) corresponded to a similar decrease in protein content in $Insr^{LKO}$ liver (Figure 2C) and increased protein content in $Tsc1^{LKO}$ liver (Figure 2D). Thus, although total glucose production was normal in both models (Figure 1E), it was supported by less liver mass in $Insr^{LKO}$ mice and more liver mass in $Tsc1^{LKO}$ mice.

Deuterated water was administered, and ^{2}H enrichments were examined in plasma glucose (Table S3) to determine the relative sources of hepatic glucose production (Table S4). Total gluconeogenesis relative to liver protein was dramatically elevated in the fed and fasted states of $Insr^{LKO}$ mice on a chow diet (Figure 2E). In contrast, mTORC1 activation, due to loss of *Tsc1*, caused a reduction of gluconeogenesis in chow-fed mice (Figure 2F). Since mTORC1 activation is associated with insulin resistance, we fed $Tsc1^{LKO}$ mice an HFD for 8 weeks to test whether they are susceptible to elevations in gluconeogenesis, but they were found to be protected (Table S1). Given the role of autophagy in supporting gluconeogenesis during fasting, we explored whether fasting autophagy was impaired in $Tsc1^{LKO}$ liver by measuring the liver:body-weight ratio during fasting. Liver size decreased by 10% after 16 hr and nearly 50% after 24 hr of fasting in control mice. In contrast, $Tsc1^{LKO}$ liver size did not decrease after 16 hr and decreased only 30% after 24 hr (Figure 2G), similar to a previous report (Sengupta et al., 2010).

Tsc1 and *Insrβ* Deletion Impair Hepatic Glycogen Metabolism

Since glycogen metabolism is regulated by insulin signaling, we examined whether loss of insulin action or gain of mTORC1 function altered the ability of the liver to store or utilize glycogen (Figure 3). Glycogen content was reduced in fed $Insr^{LKO}$ liver (Figure 3A), as expected, but was also reduced in $Tsc1^{LKO}$ mice (Figure 3B). In vivo glycogenolysis measured by ^{2}H incorporation into plasma glucose (Tables S1, S2, and S3) was normal in $Insr^{LKO}$ mice (Figure 3C) but was reduced by 50% in $Tsc1^{LKO}$ mice (Figure 3D) on a chow diet relative to liver protein. An HFD for 8 weeks increased the effect in $Tsc1^{LKO}$ mice so that whole body glucose production via glycogenolysis was decreased, even despite larger liver mass (Table S1). We confirmed reduced glycogen breakdown in HFD $Tsc1^{LKO}$ mice by measuring liver glycogen content over 16 hr of fasting (Figure 3E).

To further examine the mechanism of altered glycogen metabolism, mice were fed a high sucrose diet (HSD) to promote glycogen synthesis and were studied in the fasted and refed states. The normal rise in plasma glucose following refeeding was exacerbated in $Insr^{LKO}$ (Figure 3F) but not in $Tsc1^{LKO}$ mice (Figure 3G). Both $Insr^{LKO}$ and $Tsc1^{LKO}$ mice had reduced glycogen deposition after refeeding (Figures 3H and 3I). Western blot analysis indicated that Akt phosphorylation ($pAkt_{S473}$) and mTORC1 activation assessed by S6 phosphorylation ($pS6_{S240/244}$) were induced by refeeding in control mice (Figure 3J), but deletion of *Tsc1* or *Insrβ* blunted this response. Upon refeeding of $Insr^{LKO}$ mice, *Gck* (glucokinase) mRNA remained low, while *Gys2* (liver isoform of glycogen synthase)

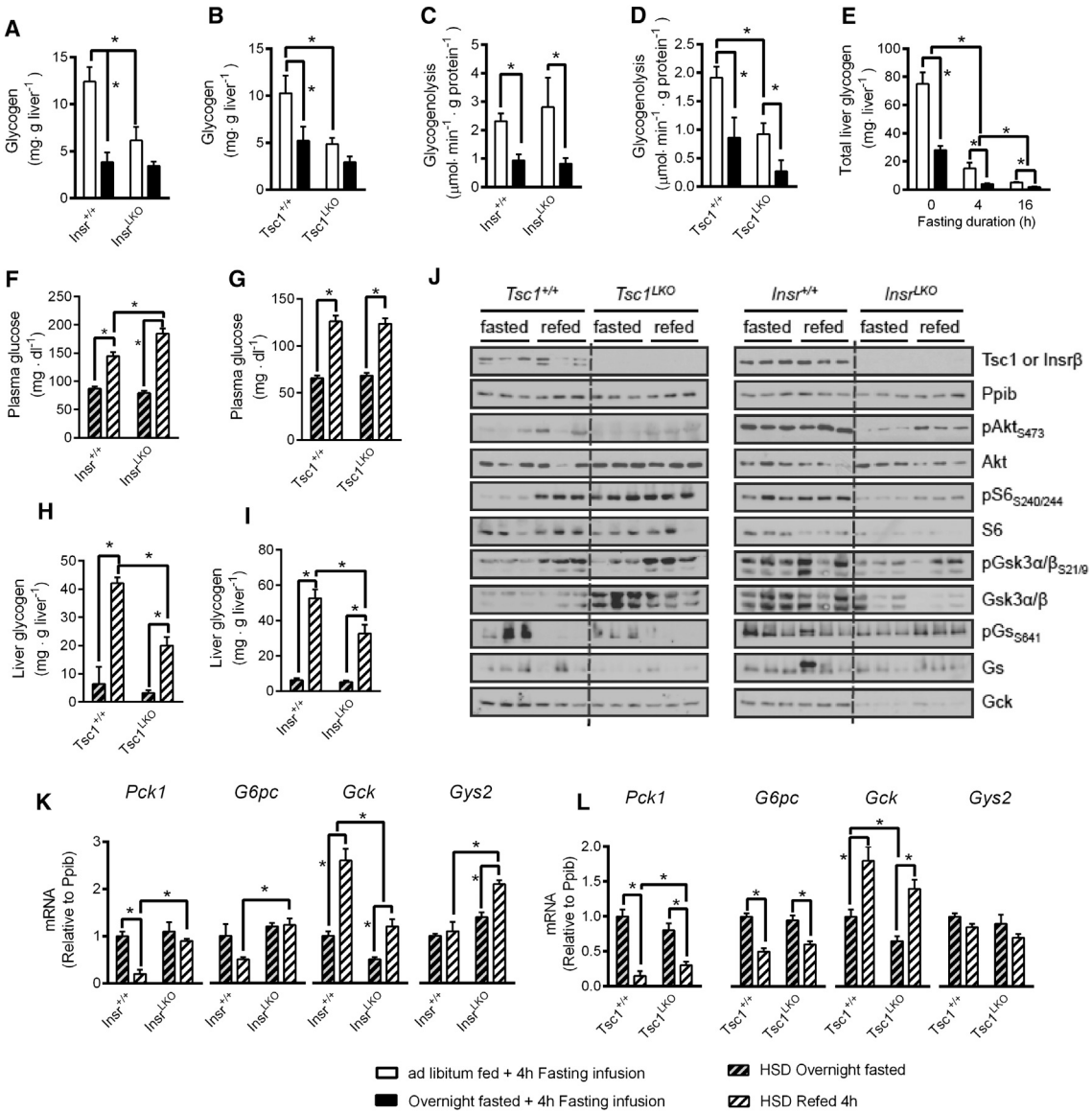

Figure 3. Glycogen Metabolism Is Altered in Livers with Short-Term Inactivation of the Insulin Receptor or mTORC1 Activation

(A–E) Mice on a chow diet (n = 4–7) were fed ad libitum or overnight (17 hr) fasted.

(A and B) Liver glycogen content in *Insr*^{LKO} (A) and *Tsc1*^{LKO} (B) mice.

(C and D) In vivo glycogenolysis in *Insr*^{LKO} (C) and *Tsc1*^{LKO} (D) mice was measured by ^{2}H incorporation into plasma glucose H2 and H5.

(E) Glycogen depletion was measured in *Tsc1*^{LKO} mice over a 16-hr fast.

(F–I) Animals fed a high sucrose diet (HSD) for 10 days were examined (n = 5–9) after an overnight fast (17 hr) or refeeding (4 hr) for plasma glucose (F and G) and liver glycogen (H and I).

(J) Western blot analysis in liver lysates from a subset of animals.

(K and L) mRNA levels of genes related to glycogen metabolism quantified by qRT-PCR.

Data are expressed as the mean and SE, with significant differences determined by unpaired two-tailed Student's t test assuming equal variances and identified as *$p < 0.05$.

mRNA was upregulated in *Insr*^{LKO} livers (Figure 3K). The effects on gene expression were more modest in *Tsc1*^{LKO} mice; Gck was low in the fasted state but was not significantly lower in the fed state (Figure 3L). Nevertheless, glucokinase and glycogen synthase proteins were low in *Tsc1*^{LKO} livers (Figure 3J). Glycogen synthase kinase (Gsk3α/β) protein phosphorylation responded normally to refeeding, but total protein content was remarkably elevated in *Tsc1*^{LKO} livers. Consistent with low *Gck* mRNA expression in *Insr*^{LKO}, glucokinase protein levels were dramatically reduced (Figure 3J), without a change in the level of glucokinase regulatory protein (data not shown). Liver glycogen synthase protein in refed *Insr*^{LKO} mice remained

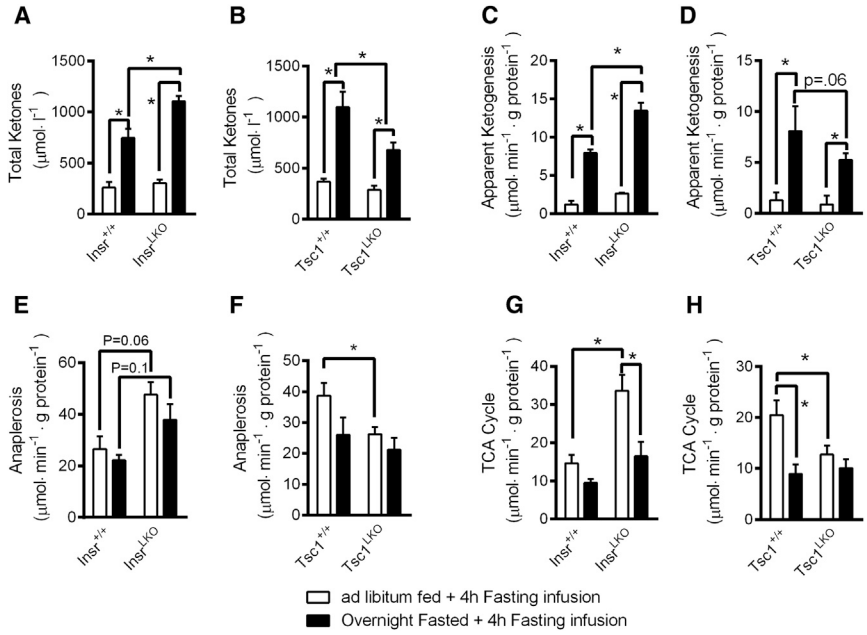

Figure 4. Hepatic Mitochondrial Fluxes Are Induced by Loss of Insulin Action but Suppressed by mTORC1 Activation

Mice on a chow diet (n = 4–7) were fed ad libitum or overnight (17 hr) fasted.

(A and B) Plasma ketones in $Insr^{LKO}$ (A) and $Tsc1^{LKO}$ (B) mice.

(C and D) Apparent ketogenesis measured by tracer dilution of [3,4-$^{13}C_2$]acetoacetate and [U-$^{13}C_4$]β-hydroxybutyrate in $Insr^{LKO}$ (C) and $Tsc1^{LKO}$ (D) mice.

(E–H) Anaplerosis measured in $Insr^{LKO}$ (E) and $Tsc1^{LKO}$ (F) mice and TCA cycle flux in $Insr^{LKO}$ (G) and $Tsc1^{LKO}$ (H) mice measured by ^{13}C and ^{2}H nuclear magnetic resonance (NMR) isotopomer analysis of plasma glucose.

Data are expressed as the mean and SE, with significant differences determined by unpaired two-tailed Student's t test assuming equal variances and identified as *$p < 0.05$.

phosphorylated (inactive) following refeeding (Figure 3J). Gsk3α/β phosphorylation responded normally to refeeding in $Insr^{LKO}$ mice, but in contrast to $Tsc1^{LKO}$ livers, total protein was very low, suggesting that glycogen synthase phosphorylation may be instigated by some other mechanism(s). Thus, insulin receptor loss of function and over-activation of mTORC1 reduce hepatic glycogen synthesis through distinct mechanisms. Changes in mRNA, protein, and phosphorylation levels in $Insr^{LKO}$ liver are consistent with impaired glycogen synthesis due to inactivation of glycogen synthase and low glucokinase content, but reduced glycogen stores in $Tsc1^{LKO}$ livers may be related to dramatically reduced Gs protein content.

Tsc1 and *Insrβ* Deletion Have Opposite Effects on Mitochondrial Metabolism

Insulin resistance impinges on oxidative metabolism and mitochondrial function; therefore, we examined in vivo fluxes through mitochondrial pathways (Figure 4). Ketogenesis occurs predominantly in liver mitochondria by the β-oxidation of fatty acids and is induced by fasting. Plasma ketones were elevated in chow-fed $Insr^{LKO}$ mice (Figure 4A) but reduced during fasting in $Tsc1^{LKO}$ mice (Figure 4B). Likewise, when ^{13}C-labeled ketones were infused into conscious unrestrained mice, the apparent turnover of acetoacetate and β-hydroxybutyrate were increased in $Insr^{LKO}$ mice (Figure 4C) but decreased in $Tsc1^{LKO}$ mice (Figure 4D). This finding was not dependent on normalization to liver protein (Tables S1 and S2). To examine in vivo mitochondrial metabolism, ^{13}C tracers of the hepatic TCA cycle were also infused, and isotopomer analysis of glucose was performed (Tables S5 and S6). Consistent with changes in gluconeogenesis, anaplerosis, or the nonoxidative flux of carbon into the TCA cycle (e.g., pyruvate carboxylation, glutaminolysis, etc.), was increased by 50% in fed $Insr^{LKO}$ mice (Figure 4E) and decreased by 35% in fed $Tsc1^{LKO}$ mice on a chow diet (Figure 4F). Oxidative metabolism in the TCA cycle was generally decreased by fasting (Figures 4G and 4H), consistent with a recent study using similar methodology (Hasenour et al., 2015). $Insr^{LKO}$ mice had an overall increase in hepatic TCA cycle flux but remained responsive to the nutritional state (Figure 4G). In contrast, hepatic TCA cycle flux in $Tsc1^{LKO}$ mice was reduced and unresponsive to the nutritional state (Figure 4H).

We examined several factors that might contribute to lower oxidative metabolism in the liver of HFD $Tsc1^{LKO}$ mice (Figure 5). Neither NEFAs (nonesterified fatty acids) (Figure 5A) nor mitochondrial content evaluated by homogenate citrate synthase (Cs) activity relative to liver mass were reduced in $Tsc1^{LKO}$ mice (Figure 5B). However, expression of several hepatic genes that regulate fat oxidation, including Pparα, *Cpt1*, and *Hmgcs2*, were lower in in $Tsc1^{LKO}$ livers (Figure 5C). In contrast, *Acacb* mRNA was increased ~2-fold, and *Mcd* mRNA was decreased ~2-fold (Figure 5C). These two enzymes catalyze the synthesis and degradation of malonyl-coenzyme A (CoA), an inhibitor of Cpt1-mediated lipid transport into the mitochondria. Total Acc protein, but not phosphorylation, tended to be increased (Figures 5D–5E). In addition, when refed mice were treated with rapamycin to inhibit mTORC1, Acc phosphorylation was robustly increased (Figure 5F), confirming that mTORC1 impinges directly or indirectly on Acc. Although malonyl-CoA concentration was not increased (Figure 5G), malonylcarnitine (C3DC/C5OH, includes 3-hydroxy-isovalerylcarnitine) was significantly, though modestly, elevated in the liver of fasted $Tsc1^{LKO}$ mice (Figure 5H). To directly test whether β-oxidation is impaired, $Tsc1^{LKO}$ liver homogenates from fasted HFD animals were exposed to [1-^{14}C]palmitate and found to have a clear reduction in ^{14}C metabolites (Figure 5I), consistent with reduced in vivo ketogenesis (Figure 4D) and an overall reduction in β-oxidation. Thus, mTORC1 activation appears to suppress fat oxidation in vitro and in vivo by reducing the expression of oxidative genes and, possibly, by inhibiting Acc phosphorylation.

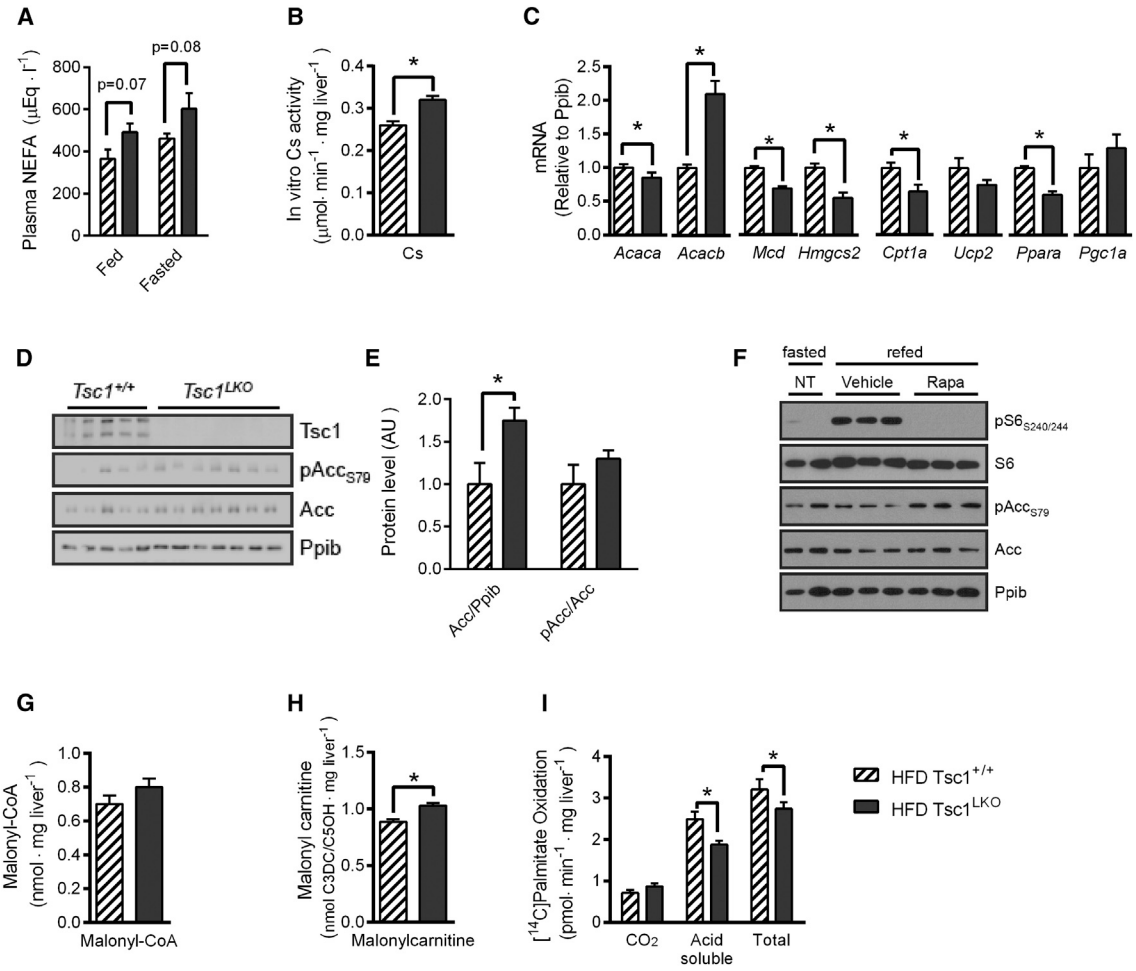

Figure 5. Activation of mTORC1 in *Tsc1*^{LKO} Mice Suppresses Mechanisms of Fat Oxidation

(A–I) Mice on an HFD for 8 weeks (n = 4–7) were fed ad libitum or overnight (17 hr) fasted.

(A) Plasma NEFAs.

(B) Mitochondrial content assessed by CS activity in tissue homogenate.

(C) qRT-PCR analysis of genes related to fat oxidation.

(D) Western blot analysis in liver lysates from a subset of animals.

(E) Quantification of Acc and pAcc.

(F) Stimulation of Acc phosphorylation by rapamycin-induced mTORC1 inhibition.

(G) In vitro [1-^{14}C]palmitate oxidation.

(H and I) Hepatic malonyl-CoA (H) and malonylcarnitine (I).

Data are expressed as the mean and SE, with significant differences determined by unpaired two-tailed Student's t test assuming equal variances and identified as *$p < 0.05$.

Simultaneous Loss of Insulin Action and Activation of mTORC1 Recapitulate Some Metabolic Features of Insulin Resistance

Moderate-duration (6–8 weeks) HFD models have relatively few overt metabolic disturbances but eventually develop hyperglycemia, defects in glycogen metabolism, impaired β-oxidation, and ketogenesis, with more severe obesity and insulin resistance. Since continued activation of mTORC1 during insulin resistance may play a role in altered hepatic metabolism (Li et al., 2010), we examined *Insr*^{LKO},*Tsc1*^{LKO} (*Insr*/*Tsc1*^{DLKO}) mice on an HFD for 8 weeks to determine whether stimulation of mTORC1 in the setting of impaired insulin action recapitulates severe diet-induced insulin resistance (Figure 6). *Insr*/*Tsc1*^{DLKO} mice had body weights similar to those of *Insr*^{LKO}/*Tsc1*$^{+/+}$ and *Insr*$^{+/+}$/*Tsc1*^{LKO} mice. Loss of *Tsc1* at least partially rescued the smaller liver size associated with loss of *Insrβ* (Figure 6A), indicating that activation of mTORC1 is sufficient to stimulate growth. Insulin levels were not reduced in *Insr*/*Tsc1*^{DLKO} mice compared to *Insr*^{LKO}/*Tsc1*$^{+/+}$ mice (Figure 6B). Liver triglyceride concentration was reduced in *Insr*$^{+/+}$/*Tsc1*^{LKO}, as previously reported (Kenerson et al., 2015), and was also reduced in *Insr*/*Tsc1*^{DLKO} mice compared to *Insr*^{LKO}/*Tsc1*$^{+/+}$, indicating that the reduction in liver triglycerides was independent of insulin action (Figure 6C). To evaluate hepatic fat oxidation, we examined

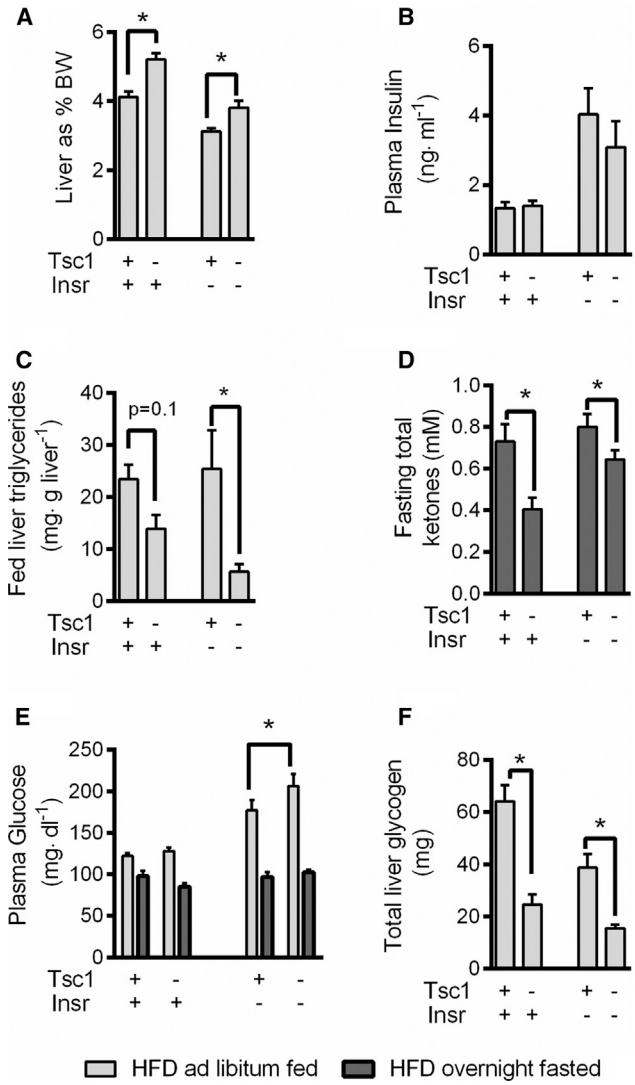

Figure 6. Simultaneous Loss of Insulin Action and Activation of mTORC1 Reduced Ketogenesis, Provoked Hyperglycemia, and Severely Impaired Glycogen Storage

Double *Insr/Tsc1* LKO mice were made by crossing *Tsc1*$^{f/+}$ and *Insr*$^{f/f}$ mice. Mice were fed an HFD for 8 weeks and treated with Ad-Cre 2 weeks prior to sample collection. The (–) designates that the gene was floxed or (+) not floxed. Mice were fed ad libitum or overnight fasted (n = 6–9).

(A) Percent liver weight compared to body weight (BW).

(B) Plasma insulin.

(C) Liver triglyceride content.

(D) Plasma total ketone concentration.

(E) Plasma glucose.

(F) Liver glycogen content.

Data are expressed as the mean and SE, with significant differences determined by unpaired two-tailed Student's t test assuming equal variances and identified as *$p < 0.05$.

fasting plasma ketone concentration. In agreement with reduced ketogenesis caused by activation of mTORC1 (Table S1), both *Insr*$^{+/+}$/*Tsc1*^{LKO} mice and *Insr/Tsc1*^{DLKO} mice had low ketone concentration (Figure 6D). In contrast to the effects on ketogenesis, fed glucose in *Insr/Tsc1*^{DLKO} mice was elevated compared to *Insr*^{LKO}/*Tsc1*$^{+/+}$ (Figure 6E). Although gluconeogenesis was not measured in *Insr/Tsc1*^{DLKO} mice, absolute endogenous gluconeogenesis (not normalized to liver protein) was not elevated in fasted or fed *Tsc1*^{LKO} or *Insr*^{LKO} mice (Tables S1 and S2). In contrast, liver glycogen storage in fed mice was impaired in *Insr*^{LKO}/*Tsc1*$^{+/+}$ mice and further impaired in *Insr/Tsc1*^{DLKO} mice (Figure 6F). These data are consistent with distinct mechanisms of impaired glycogen metabolism caused by loss of insulin action and gain of mTORC1 function and suggest that impaired glycogen storage is involved in the aggravation of hyperglycemia in the *Insr/Tsc1*^{DLKO} mice.

An HFD for 8 Weeks Activates mTORC1 and Suppresses TCA Cycle Flux in Liver of Fed Mice

We previously reported that 16 weeks, but not 8 weeks, of an HFD caused elevated fasting hepatic TCA cycle flux (Satapati et al., 2012), partially due to elevated anaplerosis and gluconeogenesis (Satapati et al., 2015). Since mTORC1 is nutritionally regulated, we examined whether its role in meditating dysregulated metabolism during an HFD is dependent on nutritional state (Figure 7). An HFD for 16 weeks was sufficient to cause increased mTORC1 activity, as indicated by elevated pS6/S6, particularly in the fed state (Figure 7A). As in our previous study (Satapati et al., 2012), 8 weeks of an HFD had no effect on oxidative fluxes in fasted mice. However, flux through the TCA cycle was significantly diminished in the fed state of mice on an HFD (Figure 7B). Activation of mTORC1 in chow-fed *Tsc1*^{LKO} mice caused a similar reduction of TCA cycle flux, which was not further decreased by an HFD (Figure 7B). In contrast, 8 weeks of an HFD had no effect on ketogenesis in control mice (Figure 7C), similar to our previous report (Sunny et al., 2010), but caused a reduction in ketogenesis when mTORC1 was constitutively active (Figure 7C). Thus, 8 weeks of an HFD or activation of mTORC1 similarly suppressed TCA cycle oxidative flux in the fed mice and together potentiated impaired β-oxidation in the fasted state.

DISCUSSION

The complex signaling network of mTor kinase integrates a plethora of positive and negative regulatory events for cell growth, replication, survival, aging, and metabolism (Laplante and Sabatini, 2013). mTORC1 is an important downstream node of the insulin signaling pathway and, hence, is expected to govern certain features of insulin action. These features are presumed to be dominated by anabolic pathways like growth, protein synthesis, and lipid synthesis. However, mTORC1 also participates in the pathophysiology of insulin resistance. Hepatic mTORC1 is over-activated in obese rodents (Figure 7A) (Khamzina et al., 2005) and may induce a negative-feedback loop from S6K1 to IRS1 (Harrington et al., 2004) and worsen insulin signaling. Constitutive activation of mTORC1 during hyperinsulinemia may also mediate the paradoxical activation of lipid synthesis through downstream targets that activate Srebp (Li et al., 2010). However, long-term mTor inhibition with rapamycin also induces a metabolic syndrome, including insulin resistance, glucose intolerance, and dyslipidemia (Laplante and Sabatini, 2012). In mice, 2 weeks of rapamycin treatment decreases expression of insulin signaling proteins in muscle (Blättler et al.,

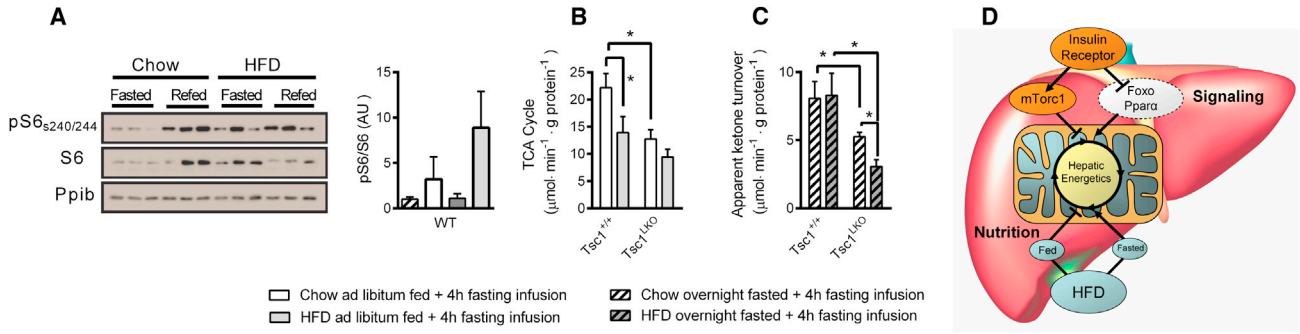

Figure 7. An HFD Activates mTORC1 and Suppresses TCA Cycle Flux in Liver of Fed Mice

(A) Western blot and quantification of S6 phosphorylation and total S6 as indicated by mTORC1 activation during an HFD.

(B and C) TCA cycle flux in fed (B) and ketogenesis in fasted (C) $Tsc1^{+/+}$ and $Tsc1^{LKO}$ on either chow or an HFD (n = 4–7).

(D) Effects of loss of insulin action, mTORC1 activation, and/or HFD on mitochondrial metabolism.

Data are expressed as the mean and SE, with significant differences determined by unpaired two-tailed Student's t test assuming equal variances and identified as *$p < 0.05$.

2012) and inhibits assembly of both mTORC1 and mTORC2 in various tissues, with the latter playing an important role in hyperinsulinemia, systemic insulin resistance, and glucose intolerance (Lamming et al., 2012). Nevertheless, very long (20-week) rapamycin treatment (Fang et al., 2013) or genetic inactivation of mTORC1 activity improves insulin sensitivity and hyperglycemia in mice (Völkers et al., 2014). Thus, while well studied, the interaction of mTORC1 with the metabolic actions of insulin is complex; varies between acute and chronic action; and is, overall, still poorly understood.

Although an HFD impairs hepatic insulin action, it also activates mTORC1, yet conditional loss of insulin signaling or activation of mTORC1 had opposite effects on liver metabolism. mTORC1 activation by hepatic *Tsc1* ablation for up to 8 weeks does not increase plasma glucose concentration in mice (Kenerson et al., 2011; Sengupta et al., 2010). $Tsc1^{LKO}$ animals repressed G6pase normally (and *Pck1* partially) in response to refeeding and had reduced fasting gluconeogenic flux on an HFD but not on a chow diet. Loss of the insulin receptor for 2 weeks caused the failed repression of hepatic G6pase and Pck1 and very low *Gck* upon refeeding, an effect that is similar to that in fed LIRKO mice (Michael et al., 2000), but endogenous glucose production was not increased. Thus, $Insr^{LKO}$ mice exhibited a phenotype similar to that of young LIRKO animals, which were reported to have hyperinsulinemia but normoglycemia for up to 4 weeks of age (Okada et al., 2007).

Activation of mTORC1 can suppress gluconeogenesis via at least two potential mechanisms. Phosphorylation and activation of S6k by mTORC1 induces the phosphorylation of Pgc1 at sites that render it unable to activate gluconeogenic genes via HNF4α but preserve its ability to maintain mitochondrial biogenesis (Lustig et al., 2011). Indeed, gluconeogenic genes were reduced in $Tsc1^{LKO}$ liver. In addition, reduced gluconeogenesis in newborn mice with activation of mTORC1 was previously attributed to inhibition of autophagy and restricted supply of amino acids for gluconeogenesis (Efeyan et al., 2013). Amino acid levels trended lower in 24-hr-fasted $Tsc1^{LKO}$ animals on an HFD (data not shown), and loss of liver mass during fasting was substantially delayed. In agreement with the established role of insulin action and mTORC1 in tissue growth, $Tsc1^{LKO}$ mice had increased total liver protein, while $Insr^{LKO}$ mice had decreased total liver protein. Liver mass was also an important factor influencing metabolic flux in a practical sense. Total absolute flux (μmol · min^{-1}) was only modestly altered in some instances in either $Tsc1^{LKO}$ or $Insr^{LKO}$ mice. However, since liver mass was markedly increased by mTORC1 activation and decreased by insulin receptor loss, striking effects were observed in functional hepatocellular fluxes (μmol · min^{-1} · g liver $protein^{-1}$).

Despite having opposite effects on gluconeogenesis, both loss of the insulin receptor and activation of mTORC1 reduced rates of glycogenolysis and glycogen synthesis. The role of insulin action on hepatic glycogenolysis is expected (Buettner et al., 2005), but the role of mTORC1 in hepatic glycogen metabolism is less appreciated. However, several mechanisms link mTORC1 activation to impaired glycogen metabolism. First, blunted Akt phosphorylation may contribute to low hepatic glycogen in both $Tsc1^{LKO}$ and $Insr^{LKO}$ mice via Gsk3-dependent and -independent mechanisms (Wan et al., 2013). Indeed, this appears to be the case in $Insr^{LKO}$ mice, which had low total and phosphorylated Gsk3 and failed to dephosphorylate glycogen synthase (Gs) after refeeding. This mechanism appears less important in $Tsc1^{LKO}$ mice, which maintained Gsk3 regulation. Second, mTORC1 was recently reported to activate glycogen synthesis through Srebp-mediated regulation of protein-targeting glycogen (PTG) (Lu et al., 2014). Indeed, mTORC1 activation paradoxically reduced *Srebp-1c* mRNA by more than 2-fold (data not shown). Finally, the most prominent defect related to glycogen in $Tsc1^{LKO}$ mice was not Gs phosphorylation but, rather, a substantial reduction in Gs protein content. Indeed, glycogen metabolism is additive in the *Insrβ*/*Tsc1* DLKO, consistent with independent mechanisms by which $Tsc1^{LKO}$ and $Insr^{LKO}$ perturb glycogen metabolism.

Like hepatic glucose metabolism, hepatic mitochondrial metabolism is also nutritionally responsive and partially regulated through insulin signaling mechanisms. Fasting caused a suppression of TCA cycle flux, similar to findings of a recent study (Hasenour et al., 2015). We tested whether loss of insulin action

and/or constitutive activation of mTORC1 are individually sufficient to modulate mitochondrial oxidative metabolism. The loss of insulin receptor increased in vivo hepatic oxidative metabolism, evident as elevated oxidative TCA cycle flux in fed mice and elevated ketogenesis in fasted mice. The activation of mTORC1 had a strikingly opposite effect by suppressing TCA cycle oxidative flux in the fed state and ketogenic flux in the fasted state. The suppression of hepatic ketogenesis by activation of mTORC1 is thought to involve repression of *Ppar*α through the activation of nuclear receptor co-repressor 1 and downregulation of *Hmgcs2* (Sengupta et al., 2010), a critical enzyme in ketogenesis. Indeed, we found that mTORC1 activation induced Pparα oxidative target genes, including *Hmgcs2*. In addition, *Acc2* mRNA and protein content were increased, but *Mcd* was reduced, which may induce malonyl-CoA levels in the vicinity of mitochondria and suppress Cpt1-mediated fat transport into mitochondria (McGarry, 2002). It is interesting that fasting reduces TCA cycle flux but loss of insulin action (a fasting-like state) increases and that mTORC1 activation (a fed-like state) suppresses TCA cycle flux. Perhaps it is most notable that constitutive activation of mTORC1 ablated the nutritional responsiveness of hepatic energy metabolism, as observed by the blunted TCA cycle flux in fed mice and no further reduction by fasting. On the other hand, the loss of the insulin receptor elevated oxidative fluxes regardless of nutritional state, but the decrement due to fasting was retained. Thus, mTORC1 deactivation, but not necessarily insulin action per se, is required for nutritional flexibility of oxidative metabolism in liver.

Since insulin resistance activates mTORC1, an HFD should recapitulate aspects of the *Tsc1*^{LKO} and *Insr*^{LKO} mice. Observations in humans and animal models indicate a spectrum of changes in hepatic mitochondrial metabolism during insulin resistance. Mild insulin resistance may have no effect, while moderate insulin resistance induces hepatic oxidative metabolism, and more severe insulin resistance is associated with defects in β-oxidation and respiration (Cheng et al., 2009; Koliaki et al., 2015; Rector et al., 2010; Satapati et al., 2008, 2012; Sunny et al., 2011). However, an important finding reported here is that the nutritional state of the subject may be as important as the degree of obesity/insulin resistance when it comes to understanding the effect on mitochondrial metabolism. For example, an HFD for 16 weeks caused increased oxidative flux in liver of fasted mice, but 8 weeks seemed to have no effect (Satapati et al., 2012). This increase could be explained by elevated anaplerosis and gluconeogenic energy demand (Satapati et al., 2015), and since 8 weeks of an HFD was not sufficient to alter these fluxes in the fasted state, an effect on mitochondrial metabolism was not observed. However, even short durations of an HFD are sufficient to cause hepatic insulin resistance, so effects on mitochondrial metabolism might be best observed in mice that are not fasted, when insulin resistance is most prominent. Indeed, the increment between fed and fasted states was essentially abolished after 8 weeks of an HFD. Thus, in fed mice, our results are similar to those of Thyfault and colleagues, who found impaired hepatic oxidative capacity in rat models susceptible to hepatic steatosis (Thyfault et al., 2009). Hence, it appears that an HFD in mice induces oxidative metabolism in the fasted state but suppresses it in the immediate post-absorptive state and, perhaps, overall reduces the nutritional flexibility of the pathway.

This "flexibility" in oxidative metabolism may be governed in part by mTORC1 activation. Activation of mTORC1 for 2 weeks closely resembles the effect of 8 weeks of an HFD, by suppressing the oxidative TCA cycle in fed mice, and resembles more severely insulin-resistant models by suppressing fasting ketogenesis. Thus, reduced oxidative mitochondrial function could precede frank insulin resistance, as previously described (Rector et al., 2010), through mTORC1 or other discrete signaling pathways activated by obesity. Severely insulin-resistant models, such as leptin-receptor-deficient rats, have a strong induction of mTor signaling (Zheng et al., 2009) and reduced hepatic fat oxidation secondary to impaired ketogenesis (Satapati et al., 2008). A similar but less severe effect is observed after a long-term (32-week) HFD (Satapati et al., 2012). The suppression of ketogenesis by mTORC1 activation may have important implications for fatty liver disease, which was recently demonstrated to progress from steatosis to steatohepatitis when ketogenesis was suppressed by *Hmgcs2* loss (Cotter et al., 2014). Thus, it is significant that, in the setting of lost insulin action, mTORC1 activation was sufficient to suppress ketogenesis and potentiate hyperglycemia, partially mediated by impaired glycogen storage.

Although we interpret the data to indicate that insulin signaling and mTORC1 activation can partially mediate the hepatic metabolic effects of diet-induced obesity, the study has several limitations. The background strains of the LKO mice were not perfectly controlled. *Insr*^{LKO} mice were purchased backcrossed, and C57bl/6J control mice were used as suggested by Jackson Laboratory (Jackson Laboratory, 2016). However, subsequent information suggests that the mice are actually C57bl/6N (Jackson Laboratory, 2016). Thus, comparison between *Insr*^{LKO} and *Tsc1*^{LKO} mice could not be made. Since DLKO mice were created by crossing heterozygous mice, those comparisons should be valid, though flux was not measured in that cohort. We also noted that, following the Ad-Cre injections 2 weeks prior to studies, mice stopped gaining weight on an HFD; thus, the weight of the mice was slightly less than usual for mice on an 8-week HFD, though they were still significantly heavier than chow-fed mice. Comparisons to control mice should be valid, since they were also administered Ad-Cre.

Finally, it has been suggested that propionate tracers of TCA cycle metabolism alter flux and yield substantially different values compared to lactate tracers (Perry et al., 2016). However, we recently validated our approach by correlating tracer flux and oxygen consumption in perfused liver, by measuring in vivo glucose production with/without propionate, and by direct comparison of propionate and lactate tracers (Satapati et al., 2015). Neither an independent group (Hasenour et al., 2015) nor we (Satapati et al., 2015) could identify substantial effects of propionate on TCA cycle flux when used at tracer levels and analyzed by an appropriate mathematical model. In fact, lactate tracers have historically reported relative fluxes similar to ours (Beylot et al., 1995; Landau et al., 1995), so we are uncertain why another group obtained very different results with lactate and other

tracers (Befroy et al., 2014; Perry et al., 2016). For the interested reader, we recommend a recent review (Previs and Kelley, 2015).

In summary, loss of insulin action and constitutive activation of mTORC1 both occur during hepatic insulin resistance. Short-term inactivation of hepatic *Tsc1* constitutively activated mTORC1 and opposed many of the metabolic effects observed in $Insr^{LKO}$ mice, with the exception of glycogen metabolism, which was suppressed by both. An 8-week HFD caused the suppression of hepatic TCA cycle flux in the fed, but not fasted, state, and this was recapitulated in chow-fed $Tsc1^{LKO}$ mice. The loss of insulin action, rather than mTORC1 activation, appears to be more directly related to the upregulation of fluxes of the TCA cycle, as observed in fasted mice after 16 weeks of an HFD. Together, insulin resistance and mTORC1 activation may account for a loss in the responsiveness of mitochondrial fluxes to nutritional state during obesity and insulin resistance.

EXPERIMENTAL PROCEDURES

Animals

All animal experiments were approved by The University of Texas Southwestern Medical Center Institutional Animal Care and Use Committee (IACUC). $Insr\beta^{flox/flox}$ (Aasum et al., 2003) mice were purchased from Jackson Laboratory, and C57BL/6J control mice were used as suggested (Jackson Laboratory, 2016). $Tsc1^{flox/flox}$ (Kwiatkowski et al., 2002) mice on a mixed background were backcrossed to C57BL/6J for three to eight generations and compared to littermate $Tsc1^{+/+}$ control animals. Double-floxed mice were generated first by crossing $Insr\beta^{flox/flox}$ with $Tsc1^{flox/+}$ mice from the third generation of backcross, and $Insr\beta^{flox/+}$ $Tsc1^{flox/+}$ offspring were then crossed with $Insr\beta^{flox/flox}$ mice to obtain $Insr\beta^{flox/flox}$ $Tsc1^{flox/+}$ *mice*. These mice were used as parents for the experimental $Insr\beta^{flox/flox}$ $Tsc1^{+/+}$ and $Insr\beta^{flox/flox}$ $Tsc1^{flox/flox}$ animals.

Male mice were 14–16 weeks old at the time of the sacrifice, maintained on 12-hr/12-hr dark/light cycle, with unrestricted access to food and water unless otherwise noted. Animals were fed standard chow (NCD; Teklad Diet 2016, Harlan Laboratories), an HFD (60% fat calories, Teklad Diet TD06414; Harlan Laboratories) for 8 weeks, or an HSD (10% fat calories, 70% sucrose calories, diet D07042201, Research Diets) for 10 days.

Ad-Cre (Gene Transfer Vector Core, University of Iowa) was expanded in HEK293T cells and purified using the Adeno-X Maxi Purification Kit (Clontech). Elution media was exchanged for 0.9% saline using a PD10 desalting column (GE Healthcare), and 1.3–1.5 × 10^9 plaque-forming units (PFUs) of virus per animal was injected into the tail vein of control and floxed mice 14 days before sacrifice.

Stable Isotope Tracer Infusions

Infusions were performed as described previously (Satapati et al., 2012). Briefly, on day 4 after surgical implantation of indwelling jugular vein catheters, mice that were either fed ad libitum or overnight (17 hr) fasted were placed in a clean cage. Unrestrained mice were infused with [3,4-$^{13}C_2$]acetoacetate and [U-$^{13}C_4$]sodium b-hydroxybutyrate as a bolus (8.8 and 6.7 μmol/hr, respectively) for 10 min, followed by 80 min of continuous infusion (3.5 and 2.7 μmol/hr, respectively). At the end of the infusion, ~50 μl of blood was collected for liquid chromatography-tandem mass spectrometry (LC-MS/MS) analysis of ketone turnover (Sunny et al., 2010). Mice then received an intraperitoneal injection of isotonic D_2O (99%; 27 μl per body weight). [U-$^{13}C_3$]propionate and [3,4-$^{13}C_2$]glucose were infused as a bolus (0.15 and 6 μmol/hr, respectively) over 10 min, followed by 80 min of continuous infusion (0.03 and 1.2 μmol/hr, respectively). After infusions, mice were anesthetized by isoflurane (Aerrane, Baxter), and blood was collected until exsanguinated by cardiac puncture. Liver was collected and flash-frozen in liquid nitrogen. Samples were stored at −80°C until further analysis. Altogether, fed mice were without food for ~4 hr, and fasted mice were without food for ~21 hr. Fluxes were evaluated as previously described (Satapati et al., 2012) and elaborated upon in the Supplemental Information.

Oxidation of Palmitate in Liver Homogenates

In vitro oxidation of palmitate was performed as described by Dohm et al. (1972), with few modifications. Briefly, overnight (16-hr)-fasted animals were anesthetized by isoflourane, and blood was collected by cardiac puncture. Liver was excised and submerged into ice-cold reaction buffer (2 mM ATP, 0.05 mM CoA, 1 mM dithiothreitol, 0.1 mM NAD^+, 1 mM DL-carnitine, 0.1 mM malate, 1 mM $MgCl_2$, 0.072 mM fatty-acid-free BSA, 100 mM sucrose, 10 mM K_2HPO_4, 80 mM KCl, 0.1 mM EDTA, 100 mM HEPES [pH 7.3]). ~500 mg of liver was homogenized in 2.5 ml of reaction buffer by 11 strokes of hand-operated Potter-Elvehjem homogenizer. Reaction was started by adding 3 μl of [1-^{14}C]palmitate (0.3 μCi; final 25 μM; PerkinElmer) to 200 μl of homogenate. The tube was immediately inserted into a vial with silicone septa containing filter paper soaked in hyamine hydroxide to capture $^{14}CO_2$. Reactions were incubated at 37°C for 4, 5, 6, and 7 min (duplicate for each time point) and terminated by injecting 100 ml of 7% (v/v) $HClO_4$. To ensure complete capture of $^{14}CO_2$, vials were left at 4°C overnight. On the next day, the reaction tube was centrifuged at 15,000 × *g* for 10 min. 200 μl of supernatant, as well as filter paper, was counted for incorporation of ^{14}C into acid-soluble molecules and $^{14}CO_2$ in 6 ml of scintillation liquid. After conversion to DPM and correction for scintillation counter efficiency, the oxidation rate was calculated as picomoles of oxidized palmitate per minute per milligram of tissue.

Blood and Tissue Analysis

Blood glucose was measured by glucometer (Accuchek, Roche Diagnostics). Analytical kits were used to determine liver and serum triglycerides (Sigma-Aldrich), plasma free fatty acids (Wako Chemicals), and total ketones (Wako Chemicals). Plasma insulin was measured using an ELISA kit (Crystal Chem).

Liver triglycerides were isolated by Folch extraction. Liver glycogen was isolated from tissue homogenized in 30% (w/v) KOH (1 ml/100 mg of tissue) and hydrolyzed in a boiling water bath for 15 min. Samples were centrifuged at 3,000 × *g* for 5 min, and 150 μl of supernatant was spotted onto a Whatman paper disc. The disc was washed twice with ice-cold 70% (v/v) ethanol, dried, submerged into 2 ml of 0.2 mg/ml amyloglucosidase in 50 mM sodium acetate (pH 4.8), and incubated at 55°C for 1 hr. 30–50 μl of reaction were used to determine glucose concentration.

Real-Time qRT-PCR

RNA was isolated using RNA Stat 60 (Tel-Test). cDNA was synthesized using 2 μg of total RNA and iScript Advanced cDNA Synthesis Kit (BioRad). PCR was run using iTaq Universal SYBR Green Supermix (BioRad) and the CFX384 Touch Real-Time PCR Detection System (BioRad).

Western Blot Analysis

Tissue was homogenized in RIPA buffer (Cell Signaling) with cOmplete protease inhibitors (Roche) followed by two 10-s sonications at 10% amplitude (Branson). Lysates were centrifuged at 21,000 × *g* for 5 min, and supernatant without fat layer was used in western blotting. Signals were detected using SuperSignal Pico chemiluminiscent substrate (Pierce, Thermo Fisher) and the ImageQuant LAS 4000 system (GE Healthcare). Antibodies were obtained from the following sources: Cell Signaling: Acc, pAcc(S79), Akt, pAkt(S473), Gs, pGs(S641), Gsk3, pGsk3(S21/9), Insrβ, S6, pS6(S240/244), Tsc1; Santa Cruz: Gck; Abcam: Ppib.

Chemicals

Stable isotope compounds were obtained from the following sources: Omicron Biochemicals: [3,4-$^{13}C_2$] glucose (98%); Isotec: [3,4-$^{13}C_2$]ethylacetoacetate and [U-$^{13}C_4$]sodium b-hydroxybutyrate (98%); Cambridge Isotopes: [U-$^{13}C_3$]propionate and [U-$^{13}C_3$]glucose. Other common chemicals were obtained from Sigma.

Statistical Analysis

All data are presented as means ± SE. Statistical analysis and graph preparation were performed in Prism 6 (GraphPad Software). Outliers were identified using a Grubb's test. The p values were calculated by unpaired two-tailed Student's t test, assuming equal variances. Statistically significant difference is marked as $*p < 0.05$.

SUPPLEMENTAL INFORMATION

Supplemental Information includes Supplemental Experimental Procedures, one figure, and six tables and can be found with this article online at http://dx.doi.org/10.1016/j.celrep.2016.06.006.

AUTHOR CONTRIBUTIONS

B.K., C.B.N., J.B., and S.C.B. designed experiments; B.K., S.S., J.D., X.F., and O.I. performed experiments; B.K., S.S., J.D., X.F., and O.I. acquired data; B.K., X.F., O.I., and S.C.B. analyzed data; J.B. provided reagents; and B.K., J.B., and S.C.B. wrote the manuscript.

ACKNOWLEDGMENTS

Support for this work was provided by NIH RO1DK078184 (S.C.B.) and P01DK058398 (S.C.B.) and by the Robert A. Welch Foundation I-1804 (S.C.B.). J.D. was supported by an educational grant from the Portuguese Foundation for Science and Technology (SFRH/BD/44294/2008).

Received: November 2, 2015
Revised: March 28, 2016
Accepted: May 25, 2016
Published: June 23, 2016

REFERENCES

Aasum, E., Hafstad, A.D., and Larsen, T.S. (2003). Changes in substrate metabolism in isolated mouse hearts following ischemia-reperfusion. Mol. Cell. Biochem. *249*, 97–103.

Befroy, D.E., Perry, R.J., Jain, N., Dufour, S., Cline, G.W., Trimmer, J.K., Brosnan, J., Rothman, D.L., Petersen, K.F., and Shulman, G.I. (2014). Direct assessment of hepatic mitochondrial oxidative and anaplerotic fluxes in humans using dynamic 13C magnetic resonance spectroscopy. Nat. Med. *20*, 98–102.

Beylot, M., Soloviev, M.V., David, F., Landau, B.R., and Brunengraber, H. (1995). Tracing hepatic gluconeogenesis relative to citric acid cycle activity in vitro and in vivo: Comparisons in the Use of [3-C]lactate, [2-C]acetate, and α-keto[3-C]isocaproate. J. Biol. Chem. *270*, 1509–1514.

Blättler, S.M., Cunningham, J.T., Verdeguer, F., Chim, H., Haas, W., Liu, H., Romanino, K., Rüegg, M.A., Gygi, S.P., Shi, Y., and Puigserver, P. (2012). Yin Yang 1 deficiency in skeletal muscle protects against rapamycin-induced diabetic-like symptoms through activation of insulin/IGF signaling. Cell Metab. *15*, 505–517.

Buettner, C., Patel, R., Muse, E.D., Bhanot, S., Monia, B.P., McKay, R., Obici, S., and Rossetti, L. (2005). Severe impairment in liver insulin signaling fails to alter hepatic insulin action in conscious mice. J. Clin. Invest. *115*, 1306–1313.

Cheng, Z., Guo, S., Copps, K., Dong, X., Kollipara, R., Rodgers, J.T., Depinho, R.A., Puigserver, P., and White, M.F. (2009). Foxo1 integrates insulin signaling with mitochondrial function in the liver. Nat. Med. *15*, 1307–1311.

Cotter, D.G., Ercal, B., Huang, X., Leid, J.M., d'Avignon, D.A., Graham, M.J., Dietzen, D.J., Brunt, E.M., Patti, G.J., and Crawford, P.A. (2014). Ketogenesis prevents diet-induced fatty liver injury and hyperglycemia. J. Clin. Invest. *124*, 5175–5190.

Dohm, G.L., Huston, R.L., Askew, E.W., and Weiser, P.C. (1972). Effects of exercise on activity of heart and muscle mitochondria. Am. J. Physiol. *223*, 783–787.

Efeyan, A., Zoncu, R., Chang, S., Gumper, I., Snitkin, H., Wolfson, R.L., Kirak, O., Sabatini, D.D., and Sabatini, D.M. (2013). Regulation of mTORC1 by the Rag GTPases is necessary for neonatal autophagy and survival. Nature *493*, 679–683.

Fang, Y., Westbrook, R., Hill, C., Boparai, R.K., Arum, O., Spong, A., Wang, F., Javors, M.A., Chen, J., Sun, L.Y., and Bartke, A. (2013). Duration of rapamycin treatment has differential effects on metabolism in mice. Cell Metab. *17*, 456–462.

Haas, J.T., Miao, J., Chanda, D., Wang, Y., Zhao, E., Haas, M.E., Hirschey, M., Vaitheesvaran, B., Farese, R.V., Jr., Kurland, I.J., et al. (2012). Hepatic insulin signaling is required for obesity-dependent expression of SREBP-1c mRNA but not for feeding-dependent expression. Cell Metab. *15*, 873–884.

Harrington, L.S., Findlay, G.M., Gray, A., Tolkacheva, T., Wigfield, S., Rebholz, H., Barnett, J., Leslie, N.R., Cheng, S., Shepherd, P.R., et al. (2004). The TSC1-2 tumor suppressor controls insulin-PI3K signaling via regulation of IRS proteins. J. Cell Biol. *166*, 213–223.

Hasenour, C.M., Wall, M.L., Ridley, D.E., Hughey, C.C., James, F.D., Wasserman, D.H., and Young, J.D. (2015). Mass spectrometry-based microassay of (2)H and (13)C plasma glucose labeling to quantify liver metabolic fluxes in vivo. Am. J. Physiol. Endocrinol. Metab. *309*, E191–E203.

Howell, J.J., Ricoult, S.J., Ben-Sahra, I., and Manning, B.D. (2013). A growing role for mTOR in promoting anabolic metabolism. Biochem. Soc. Trans. *41*, 906–912.

Iozzo, P., Bucci, M., Roivainen, A., Någren, K., Järvisalo, M.J., Kiss, J., Guiducci, L., Fielding, B., Naum, A.G., Borra, R., et al. (2010). Fatty acid metabolism in the liver, measured by positron emission tomography, is increased in obese individuals. Gastroenterology *139*, 846–856.e6.

Jackson Laboratory. (2016). Mouse strain data sheet - 006955. http://www.jax.org/strain/006955.

Kenerson, H.L., Yeh, M.M., and Yeung, R.S. (2011). Tuberous sclerosis complex-1 deficiency attenuates diet-induced hepatic lipid accumulation. PLoS ONE *6*, e18075.

Kenerson, H.L., Subramanian, S., McIntyre, R., Kazami, M., and Yeung, R.S. (2015). Livers with constitutive mTORC1 activity resist steatosis independent of feedback suppression of Akt. PLoS ONE *10*, e0117000.

Khamzina, L., Veilleux, A., Bergeron, S., and Marette, A. (2005). Increased activation of the mammalian target of rapamycin pathway in liver and skeletal muscle of obese rats: possible involvement in obesity-linked insulin resistance. Endocrinology *146*, 1473–1481.

Koliaki, C., Szendroedi, J., Kaul, K., Jelenik, T., Nowotny, P., Jankowiak, F., Herder, C., Carstensen, M., Krausch, M., Knoefel, W.T., et al. (2015). Adaptation of hepatic mitochondrial function in humans with non-alcoholic fatty liver is lost in steatohepatitis. Cell Metab. *21*, 739–746.

Kwiatkowski, D.J., Zhang, H., Bandura, J.L., Heiberger, K.M., Glogauer, M., el-Hashemite, N., and Onda, H. (2002). A mouse model of TSC1 reveals sex-dependent lethality from liver hemangiomas, and up-regulation of p70S6 kinase activity in Tsc1 null cells. Hum. Mol. Genet. *11*, 525–534.

Lamming, D.W., Ye, L., Katajisto, P., Goncalves, M.D., Saitoh, M., Stevens, D.M., Davis, J.G., Salmon, A.B., Richardson, A., Ahima, R.S., et al. (2012). Rapamycin-induced insulin resistance is mediated by mTORC2 loss and uncoupled from longevity. Science *335*, 1638–1643.

Landau, B.R., Chandramouli, V., Schumann, W.C., Ekberg, K., Kumaran, K., Kalhan, S.C., and Wahren, J. (1995). Estimates of Krebs cycle activity and contributions of gluconeogenesis to hepatic glucose production in fasting healthy subjects and IDDM patients. Diabetologia *38*, 831–838.

Laplante, M., and Sabatini, D.M. (2012). mTOR signaling in growth control and disease. Cell *149*, 274–293.

Laplante, M., and Sabatini, D.M. (2013). Regulation of mTORC1 and its impact on gene expression at a glance. J. Cell Sci. *126*, 1713–1719.

Li, S., Brown, M.S., and Goldstein, J.L. (2010). Bifurcation of insulin signaling pathway in rat liver: mTORC1 required for stimulation of lipogenesis, but not inhibition of gluconeogenesis. Proc. Natl. Acad. Sci. USA *107*, 3441–3446.

Lin, H.V., and Accili, D. (2011). Hormonal regulation of hepatic glucose production in health and disease. Cell Metab. *14*, 9–19.

Lu, B., Bridges, D., Yang, Y., Fisher, K., Cheng, A., Chang, L., Meng, Z.X., Lin, J.D., Downes, M., Yu, R.T., et al. (2014). Metabolic crosstalk: molecular links between glycogen and lipid metabolism in obesity. Diabetes *63*, 2935–2948.

Lustig, Y., Ruas, J.L., Estall, J.L., Lo, J.C., Devarakonda, S., Laznik, D., Choi, J.H., Ono, H., Olsen, J.V., and Spiegelman, B.M. (2011). Separation of the gluconeogenic and mitochondrial functions of PGC-1alpha through S6 kinase. Genes Dev. *25*, 1232–1244.

Mantena, S.K., Vaughn, D.P., Andringa, K.K., Eccleston, H.B., King, A.L., Abrams, G.A., Doeller, J.E., Kraus, D.W., Darley-Usmar, V.M., and Bailey, S.M. (2009). High fat diet induces dysregulation of hepatic oxygen gradients and mitochondrial function in vivo. Biochem. J. *417*, 183–193.

McGarry, J.D. (2002). Banting lecture 2001: dysregulation of fatty acid metabolism in the etiology of type 2 diabetes. Diabetes *51*, 7–18.

Michael, M.D., Kulkarni, R.N., Postic, C., Previs, S.F., Shulman, G.I., Magnuson, M.A., and Kahn, C.R. (2000). Loss of insulin signaling in hepatocytes leads to severe insulin resistance and progressive hepatic dysfunction. Mol. Cell *6*, 87–97.

Okada, T., Liew, C.W., Hu, J., Hinault, C., Michael, M.D., Krtzfeldt, J., Yin, C., Holzenberger, M., Stoffel, M., and Kulkarni, R.N. (2007). Insulin receptors in beta-cells are critical for islet compensatory growth response to insulin resistance. Proc. Natl. Acad. Sci. USA *104*, 8977–8982.

Perry, R.J., Borders, C.B., Cline, G.W., Zhang, X.M., Alves, T.C., Petersen, K.F., Rothman, D.L., Kibbey, R.G., and Shulman, G.I. (2016). Propionate increases hepatic pyruvate cycling and anaplerosis and alters mitochondrial metabolism. J. Biol. Chem. *291*, 12161–12170.

Previs, S.F., and Kelley, D.E. (2015). Tracer-based assessments of hepatic anaplerotic and TCA cycle flux: practicality, stoichiometry and hidden assumptions. Am. J. Physiol. Endocrinol. Metab. *309*, E727–E735.

Rector, R.S., Thyfault, J.P., Uptergrove, G.M., Morris, E.M., Naples, S.P., Borengasser, S.J., Mikus, C.R., Laye, M.J., Laughlin, M.H., Booth, F.W., and Ibdah, J.A. (2010). Mitochondrial dysfunction precedes insulin resistance and hepatic steatosis and contributes to the natural history of non-alcoholic fatty liver disease in an obese rodent model. J. Hepatol. *52*, 727–736.

Satapati, S., He, T., Inagaki, T., Potthoff, M., Merritt, M.E., Esser, V., Mangelsdorf, D.J., Kliewer, S.A., Browning, J.D., and Burgess, S.C. (2008). Partial resistance to peroxisome proliferator-activated receptor-alpha agonists in ZDF rats is associated with defective hepatic mitochondrial metabolism. Diabetes *57*, 2012–2021.

Satapati, S., Sunny, N.E., Kucejova, B., Fu, X., He, T.T., Méndez-Lucas, A., Shelton, J.M., Perales, J.C., Browning, J.D., and Burgess, S.C. (2012). Elevated TCA cycle function in the pathology of diet-induced hepatic insulin resistance and fatty liver. J. Lipid Res. *53*, 1080–1092.

Satapati, S., Kucejova, B., Duarte, J.A., Fletcher, J.A., Reynolds, L., Sunny, N.E., He, T., Nair, L.A., Livingston, K., Fu, X., et al. (2015). Mitochondrial metabolism mediates oxidative stress and inflammation in fatty liver. J. Clin. Invest. *125*, 4447–4462.

Sengupta, S., Peterson, T.R., Laplante, M., Oh, S., and Sabatini, D.M. (2010). mTORC1 controls fasting-induced ketogenesis and its modulation by ageing. Nature *468*, 1100–1104.

Shimomura, I., Matsuda, M., Hammer, R.E., Bashmakov, Y., Brown, M.S., and Goldstein, J.L. (2000). Decreased IRS-2 and increased SREBP-1c lead to mixed insulin resistance and sensitivity in livers of lipodystrophic and ob/ob mice. Mol. Cell *6*, 77–86.

Sunny, N.E., Satapati, S., Fu, X., He, T., Mehdibeigi, R., Spring-Robinson, C., Duarte, J., Potthoff, M.J., Browning, J.D., and Burgess, S.C. (2010). Progressive adaptation of hepatic ketogenesis in mice fed a high-fat diet. Am. J. Physiol. Endocrinol. Metab. *298*, E1226–E1235.

Sunny, N.E., Parks, E.J., Browning, J.D., and Burgess, S.C. (2011). Excessive hepatic mitochondrial TCA cycle and gluconeogenesis in humans with nonalcoholic fatty liver disease. Cell Metab. *14*, 804–810.

Thyfault, J.P., Rector, R.S., Uptergrove, G.M., Borengasser, S.J., Morris, E.M., Wei, Y., Laye, M.J., Burant, C.F., Qi, N.R., Ridenhour, S.E., et al. (2009). Rats selectively bred for low aerobic capacity have reduced hepatic mitochondrial oxidative capacity and susceptibility to hepatic steatosis and injury. J. Physiol. *587*, 1805–1816.

Völkers, M., Doroudgar, S., Nguyen, N., Konstandin, M.H., Quijada, P., Din, S., Ornelas, L., Thuerauf, D.J., Gude, N., Friedrich, K., et al. (2014). PRAS40 prevents development of diabetic cardiomyopathy and improves hepatic insulin sensitivity in obesity. EMBO Mol. Med. *6*, 57–65.

Wan, M., Leavens, K.F., Hunter, R.W., Koren, S., von Wilamowitz-Moellendorff, A., Lu, M., Satapati, S., Chu, Q., Sakamoto, K., Burgess, S.C., and Birnbaum, M.J. (2013). A noncanonical, GSK3-independent pathway controls postprandial hepatic glycogen deposition. Cell Metab. *18*, 99–105.

Zheng, Y., Zhang, W., Pendleton, E., Leng, S., Wu, J., Chen, R., and Sun, X.J. (2009). Improved insulin sensitivity by calorie restriction is associated with reduction of ERK and p70S6K activities in the liver of obese Zucker rats. J. Endocrinol. *203*, 337–347.

Zoncu, R., Efeyan, A., and Sabatini, D.M. (2011). mTOR: from growth signal integration to cancer, diabetes and ageing. Nat. Rev. Mol. Cell Biol. *12*, 21–35.